Two-center shell model for deformed and arbitrarily orientated nuclei

Gerhard Nuhn and Werner Scheid
Institut für Theoretische Physik der Justus-Liebig-Universität, Giessen, Federal Republic of Germany

Jae Young Park
Department of Physics, North Carolina State University, Raleigh, North Carolina 27695
(Received 15 September 1986)

A potential consisting of two ellipsoidally deformed Gaussian potentials is suggested to be used for a two-center shell model of deformed and arbitrarily orientated nuclei. The eigenenergies of the two-center Hamiltonian are calculated with a set of Nilsson wave functions concentrated around the individual nuclear centers. The two-center shell model is applied to the system $^{13}C+^{16}O\rightarrow^{29}Si$, where the ^{13}C nucleus is assumed to have an oblately deformed shape. Consequences for reactions between deformed nuclei resulting from the level diagrams are discussed.

I. INTRODUCTION

Two-center shell models (TCSM's) have an extensive range of application in nuclear physics. In this field of physics they were introduced, in practice, by the Frankfurt group.[1–3] Besides the application for nuclear fission and for reactions between heavier heavy ions (for a review, see Ref. 4) they were also used for the description of light heavy ion reactions within molecular reaction theories.[5–11]

Up to now the calculations in the TCSM were done with two-center potentials, which are rotationally symmetric about the internuclear axis.[2,3] Such potentials are suitable for the description of two spherical or deformed nuclei with intrinsic symmetry axes which lie along the internuclear axis. The resulting rotationally symmetric shapes of the TCSM potential are favorable for the description of fission processes, but not for heavy ion reactions between deformed nuclei. In the latter case all orientations of the intrinsic symmetry axes with respect to the internuclear axis are possible and have to be treated properly.

In this paper we present a new TCSM for arbitrary orientations of the intrinsic symmetry axes of the deformed nuclei. We suggest building up of the TCSM potential by means of two ellipsoidally deformed Gaussian potentials centered at the centers of the nuclei. TCSM potentials of spherical Gaussian type have been suggested by Hasse[12] for the description of colliding spherical nuclei. The proposed TCSM potential for deformed nuclei has several advantages: For each relative distance and orientation of the deformed nuclei a continuous and realistic two-center potential can be obtained. Also, the single-particle Hamiltonian can be conveniently diagonalized with a set of basis functions consisting of Nilsson functions centered at the nuclear centers of mass. Within this basis set all the matrix elements of the two-center potential can be calculated analytically by solving usual integrals of Gaussian type in Cartesian coordinates.

Although the new TCSM is applicable for the description of the scattering of heavier nuclei and for the calculation of potential energy surfaces for deformed nuclei within the formalism of Strutinsky, we have considered here, as an example, the application of the new TCSM to the scattering of an intrinsically oblately deformed ^{13}C nucleus on a spherical ^{16}O nucleus. This heavy ion system should be seen in relation to the observation and description of molecular single-particle effects in systems like $^{12}C+^{13}C$, $^{13}C+^{13}C$, and $^{12,13}C+^{17}O$.[11,13–18] It has been recently shown that structures observed in the inelastic cross sections and γ-ray yields of these scattering systems[14–16,19] can be understood as due to avoided level crossings of molecular single-particle states (nuclear Landau-Zener effect).[19–24] Therefore, the influence of the ^{13}C deformation on the molecular single-particle states is a quite interesting problem and should be studied for these light heavy ion reactions.

In Sec. II we discuss the Hamiltonian of the TCSM for deformed nuclei, and present the method for solving the eigenvalue problem in Sec. III. The model is applied to the system $^{13}C+^{16}O\rightarrow^{29}Si$ in Sec. IV, where we show level diagrams as functions of the relative distance and the orientation of the oblately deformed ^{13}C nucleus.

II. THE HAMILTONIAN OF THE MODEL

The neutron single-particle Hamiltonian of the TCSM consists of the kinetic energy operator and a potential for the mean interaction,

$$h_{\mathrm{TCSM}}=\frac{\mathbf{p}^2}{2M}+V(\mathbf{r},\mathbf{p},\mathbf{s})\ . \tag{1}$$

The potential is assumed to be built up as a linear superposition of two potentials including the spin-orbit potential,

$$V(\mathbf{r},\mathbf{p},\mathbf{s})=\sum_{i=1}^{2}\left[V_i+C_i(\nabla V_i\times\mathbf{p})\cdot\mathbf{s}\right]\ . \tag{2}$$

The potentials V_i are centered about $z=Z_1$ and Z_2, respectively, where the two-center distance is given by

 ©1987 The American Physical Society

$R=|Z_1-Z_2|$. These potentials are assumed to be functions of Gaussian form, which have ellipsoidal equipotential surfaces,

$$V_i=-V_{0i}\left[1+\sum_{n=1}^{n_{0i}} a_{2n}^{(i)}u_i^{2n}\right]\exp(-u_i^2),\quad i=1,2 \tag{3}$$

where

$$u_i^2=(\delta_{i1}^2x_i'^2+\delta_{i2}^2y_i'^2+\delta_{i3}^2z_i'^2)/\lambda_i^2 . \tag{4}$$

Here, $\delta_{i\mu}$ ($\mu=1,2,3$) are the deformation parameters. The coordinates (x_i',y_i',z_i') with $i=1$ and 2 are those of two intrinsic coordinate systems centered at $z=Z_1$ and Z_2, respectively, and rotated by the Eulerian angles $\Omega_i=(\phi_i,\theta_i,\psi_i)$, as shown in Fig. 1. If we introduce the coordinates $(x_{i1}',x_{i2}',x_{i3}')$ and (x_1,x_2,x_3) for (x_i',y_i',z_i') and (x,y,z), respectively, the transformation between the coordinate systems is given by

$$x_{i\mu}'=\sum_{\nu=1}^{3} R_{\mu\nu}(\Omega_i)(x_\nu-\delta_{\nu3}Z_i),\quad i=1,2 \tag{5}$$

where $R_{\mu\nu}(\Omega_i)$ are the elements of the transformation matrix depending on the Eulerian angles Ω_i.

The parameters of the potential (2) are those of the potentials (3) and the spin-orbit parameters C_i. They depend continuously on the internuclear distance R and the Eulerian angles Ω_i. The parameters V_{0i}, $a_{2n}^{(i)}$, and λ_i define the shapes of the potentials V_i and the parameters $\delta_{i\mu}$ ($i=1,2$; $\mu=1,2,3$) their ellipsoidal deformations. The spherical case ($\delta_{i\mu}=1$) was already studied by Hasse[12] with the same TCSM potential. In case of a rotationally symmetric potential about the z axis, the Eulerian angles can be chosen to be zero and the transformation (5) is not needed. For nuclei with rotationally symmetric shapes about the intrinsic z_i' axes, the deformation parameters in Eq. (4) can be related to those used in the Nilsson model,[25]

$$\delta_{i1}^2=\delta_{i2}^2=(1+\tfrac{2}{3}\delta_i)/N , \tag{6}$$

$$\delta_{i3}^2=(1-\tfrac{4}{3}\delta_i)/N , \tag{7}$$

where

$$N=(1+\tfrac{2}{3}\delta_i)^{2/3}(1-\tfrac{4}{3}\delta_i)^{1/3} . \tag{8}$$

In general, the sum over n in Eq. (3) runs only over a very few values of n and is needed to generate the correct ratio between the inner part of the potential and its surface range. Choosing $a_{2n}^{(i)}=1/n!$, one obtains potentials which are similar to those of Woods-Saxon type.

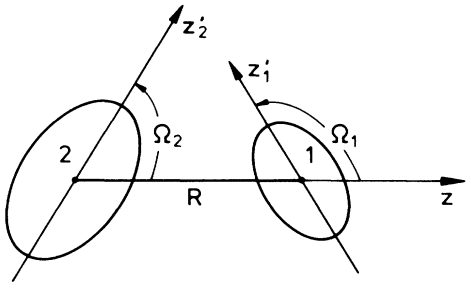

FIG. 1. Schematic picture of the coordinate systems used for the definition of the TCSM potential.

The parameters V_{0i}, $a_{2n}^{(i)}$, λ_i, $\delta_{i\mu}$, and C_i can be determined by the single-particle spectra of the nuclei for $R\to\infty$ and of the united system for $R\to0$. For overlapping nuclei the parameters have to be interpolated between their limiting values. An example for a special choice will be given in the application of the model to the system $^{13}C+{}^{16}O$ in Sec. IV. The parameters can be correlated by assuming the condition that the volume of a certain equipotential surface of V_1+V_2 is conserved for all values of R and Ω_i; namely,

$$\int d\tau\,\Theta(V_0-V_1-V_2)=v_0 , \tag{9}$$

where Θ is the Heaviside step function, V_0 a fixed potential value near the Fermi level, and v_0 the volume enclosed by the equipotential surface V_0. The volume integral in Eq. (9) can be solved only numerically and is carried out by a Monte Carlo integration method.

The potential (2) in the form (3) has several advantages. First of all, with this potential a smooth and realistic transition can be described from the potentials of the separated deformed nuclei with arbitrary oriented axes to the potential of the united system. The potentials (3) show the correct behavior ($V_i=0$) for large distances of the particles from the centers, in contrast to the oscillator-type potentials of the TCSM of Maruhn and Greiner.[3] The potential (2) yields bound and continuum states. All the matrix elements of the TCSM Hamiltonian (1) can be calculated analytically if a basis set of deformed oscillator wave functions is chosen which are centered at $z=Z_1$ and Z_2 for larger relative distances R and at the central point $z=(Z_1+Z_2)/2$ for small values of R.

III. SOLUTION OF THE TCSM PROBLEM

The eigensolutions ψ_ν of the single-particle Hamiltonian (1) can be expanded into a set of space and spin functions centered at $z=Z_1$ and Z_2 and quantized with respect to the corresponding intrinsic coordinate axes:

$$\psi_\nu=\sum_{i=1}^{2}\sum_{n,s} c_{\nu ns}^{(i)}\phi_n^{(i)}(x_i',y_i',z_i')\chi_s^{(i)} . \tag{10}$$

The functions $\phi_n^{(i)}$ are chosen as the normalized eigenfunctions of the three-dimensional oscillator

$$\phi_n^{(i)}(x_i',y_i',z_i')=\phi_{n_1}(x_{i1}',\Lambda_1^{(i)})\phi_{n_2}(x_{i2}',\Lambda_2^{(i)})\phi_{n_3}(x_{i3}',\Lambda_3^{(i)}) , \tag{11}$$

where we abbreviate the quantum numbers by

$$n=(n_1,n_2,n_3) . \tag{12}$$

The functions ϕ_n are the wave functions of the one-dimensional oscillator,

$$\phi_n(x,\Lambda)=(2^n n!\sqrt{\pi}\Lambda)^{-1/2}H_n(x/\Lambda)\exp[-x^2/(2\Lambda^2)] . \tag{13}$$

Here, H_n are the Hermite polynomials of order n, and

TABLE I. Parameters of the potentials of ^{13}C, ^{16}O, and ^{29}Si, and the oscillator energy $\hbar\omega$ used for the basis set. The parameters are defined by the potentials given in Eqs. (22) and (24).

	V_0 (MeV)	a (fm^{-2})	λ (fm)	δ	κ	$\hbar\omega$ (MeV)
^{13}C	50		3.30	−0.3	0.09	9.0
^{16}O	54.0	0.2036	2.30		0.09	12.0
^{29}Si	45.0	0.0899	3.15		0.10	9.0

Λ is the oscillator length. The oscillator lengths $\Lambda_\mu^{(i)}$ are free parameters and can be fixed for the potentials (3) in an optimum way as we show later.

The functions $\phi_n^{(i)}\chi_s^{(i)}$ are orthogonal and normalized for same values of i,

$$\langle \phi_n^{(i)}\chi_s^{(i)} \mid \phi_{n'}^{(i)}\chi_{s'}^{(i)} \rangle = \delta_{n_1 n_1'}\delta_{n_2 n_2'}\delta_{n_3 n_3'}\delta_{ss'}, \quad i=1,2 \ . \tag{14}$$

The overlaps between the functions with $i=1$ and 2 depend on R and the difference angle Ω between the Eulerian angles Ω_1 and Ω_2,

$$\langle \phi_n^{(1)}\chi_s^{(1)} \mid \phi_{n'}^{(2)}\chi_{s'}^{(2)} \rangle = N_{nn'}^{(1,2)}(R,\Omega)S_{ss'}^{(1,2)}(\Omega) \ , \tag{15}$$

where

$$N_{nn'}^{(1,2)}(R,\Omega) = \langle \phi_n^{(1)} \mid \phi_{n'}^{(2)} \rangle \ , \tag{16}$$

$$S_{ss'}^{(1,2)}(\Omega) = \langle \chi_s^{(1)} \mid \chi_{s'}^{(2)} \rangle \ . \tag{17}$$

Integrals of the form (16) are carried out by transforming the intrinsic coordinates $x'_{i\mu}$ via Eq. (5) into the laboratory coordinates x_μ and then solving the Gaussian integrals in the Cartesian coordinates x_μ. For the matrix elements over the spin states, we use the following transformation of these states to the laboratory states χ_s with $s=\pm\frac{1}{2}$:[26]

$$\chi_s^{(i)} = \sum_{s'} D_{s's}^{1/2}(\Omega_i)\chi_{s'} \ . \tag{18}$$

With this relation we obtain the spin-matrix elements (17) as

$$\langle \chi_s^{(1)} \mid \chi_{s'}^{(2)} \rangle = \sum_{s''} D_{s''s}^{1/2*}(\Omega_1)D_{s''s'}^{1/2}(\Omega_2) = D_{s's}^{1/2*}(\Omega) \ , \tag{19}$$

where $\Omega=(\phi,\theta,\phi)$ denotes the difference angles between the directions of the intrinsic coordinate systems 1 and 2.

Matrix elements of the Hamiltonian h_{TCSM} with the basis functions $\phi_n^{(i)}\chi_s^{(i)}$ can be evaluated as follows $(i,j=1,2)$:

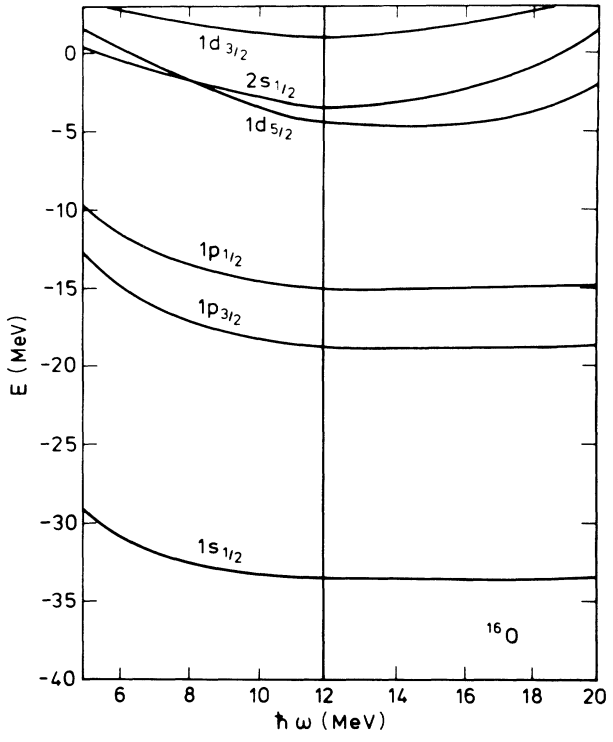

FIG. 2. The single-particle energies of ^{16}O varied as a function of $\hbar\omega$ used for the basis set including all the oscillator states up to the fourth shell ($N=3$). The value $\hbar\omega=12$ MeV has been taken in the further calculations.

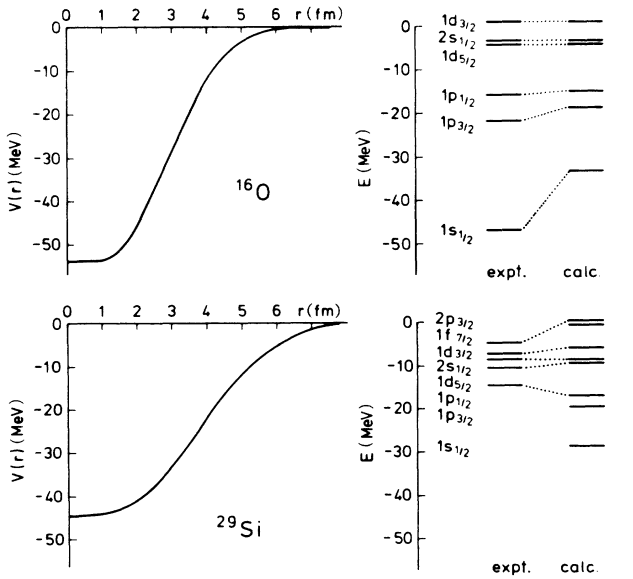

FIG. 3. The shell model potential and the experimental and calculated single-particle energies of ^{16}O and ^{29}Si.

TABLE II. The characteristic quantities of the lowest bandheads of ^{13}C, when the states are ordered in bands: E^*_{IK} and E_{IK} are the energies of the bandheads, measured with respect to the ground state and to the negative value of the separation energy of the $1p_{1/2}$ valence neutron (−4.95 MeV), respectively, their spin I, spin projection K on the body-fixed symmetry axis and parity π, the inertia parameter $\hbar^2/2J$ of the rotational energy and decoupling parameter d, the single-particle energy ϵ_Ω, calculated according to Eq. (23), and the quantum numbers of the corresponding spherical state for zero deformation.

E^*_{IK} (MeV)	E_{IK} (MeV)	I,K,π	$\hbar^2/2J$ (MeV)	d (MeV)	$\epsilon_{\Omega=K}$ (MeV)	Spherical state
0.0	−4.95	$\frac{1}{2},\frac{1}{2},-$	1.00	0.226	−4.97	$1p_{1/2}$
3.09	−1.86	$\frac{1}{2},\frac{1}{2},+$	1.18	0.282	−1.82	$2s_{1/2}$
3.85	−1.09	$\frac{5}{2},\frac{5}{2},+$	0.518		0.85	$1d_{5/2}$

$$\langle \phi_n^{(i)}\chi_s^{(i)} \mid h_{\mathrm{TCSM}} \mid \phi_{n'}^{(j)}\chi_{s'}^{(j)}\rangle = \left\langle \phi_n^{(i)} \left| \frac{\mathbf{p}^2}{2m} + V_1 + V_2 \right| \phi_{n'}^{(j)} \right\rangle \langle \chi_s^{(i)} \mid \chi_{s'}^{(j)}\rangle + \left\langle \phi_n^{(i)} \left| \sum_{k=1}^{2} C_k(\nabla V_k \times \mathbf{p}) \right| \phi_{n'}^{(j)} \right\rangle \langle \chi_s^{(i)} \mid \mathbf{s} \mid \chi_{s'}^{(j)}\rangle \ . \quad (20)$$

The space integrals may be solved by the method used for the overlaps (16), which leads to lengthy, but analytical, expressions. For the spin-matrix elements we take the transformation (18) into account and obtain

$$\langle \chi_s^{(i)} \mid \mathbf{s} \mid \chi_{s'}^{(j)}\rangle = \sum_{s_1,s_2} D^{1/2*}_{s_1 s}(\Omega_i)\langle \chi_{s_1} \mid \mathbf{s} \mid \chi_{s_2}\rangle D^{1/2}_{s_2 s'}(\Omega_j) \ . \quad (21)$$

Finally, the matrix (20) of the Hamiltonian is diagonalized with due regard to the partly nonorthogonal basis functions. Further details of the method can be found in Ref. 27.

IV. APPLICATION TO THE SYSTEM $^{13}C + ^{16}O$

In our former treatments we have calculated TCSM level diagrams for the asymmetric systems $^{12,13}C + ^{16,17}O$ and $^{16,17}O + ^{24,25}Mg$,[20,28] using the asymmetric TCSM of Maruhn and Greiner.[3] These calculations were restricted to the case of the rotational symmetry of the potentials about the internuclear axis. The TCSM potential suggested in Sec. II allows us to overcome this restrictive condition. Therefore, as the first example for the new potential, we have chosen a system consisting of a spherical and deformed nucleus. In the following we present calculations of the two-center level diagrams for the system $^{13}C + ^{16}O$, assuming that the ^{13}C nucleus is oblately deformed and the ^{16}O nucleus is spherical.

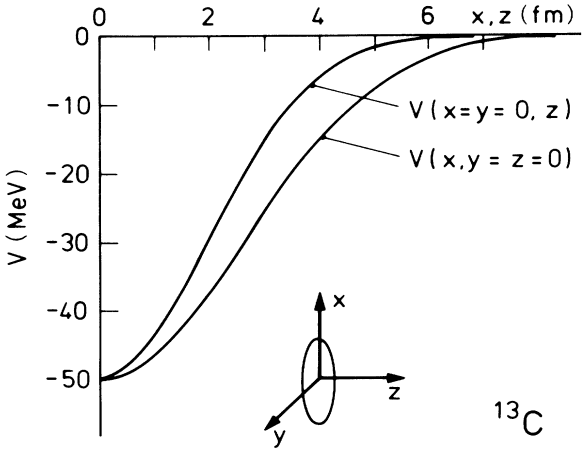

FIG. 4. The shell model potential of ^{13}C is shown along the x and z axes. The deformation parameter is $\delta = -0.3$.

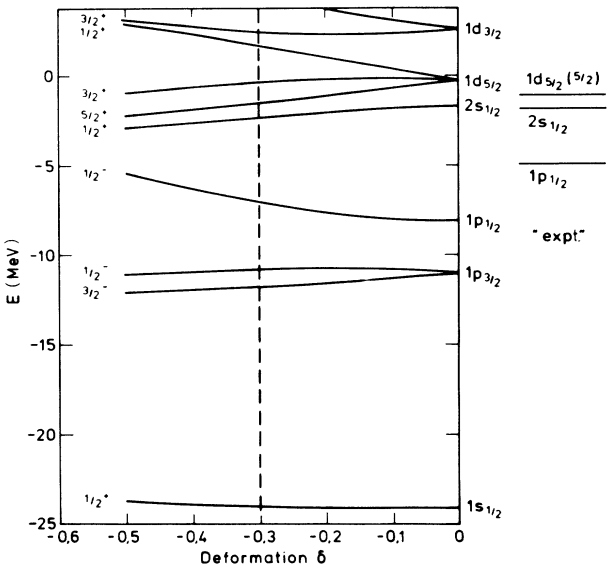

FIG. 5. Single-particle energies of ^{13}C as a function of the deformation parameter δ. The value of $\delta = -0.3$, used in the further calculations, is indicated by a dashed line. On the right-hand side the "experimental" single-particle energies are shown.

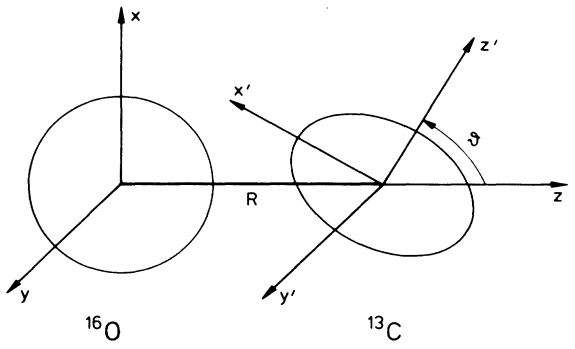

FIG. 6. Schematic picture of the $^{16}O + {}^{13}C$ system. The angle θ defines the orientation angle between the symmetry axis of the oblately deformed ^{13}C nucleus and the internuclear axis.

A. Shell model potentials for ^{16}O, ^{29}Si, and ^{13}C

In the limits $R \to 0$ and $R \to \infty$ the parameters of the TCSM potential (2) can be determined by the neutron single-particle energies of the corresponding nuclei. In our example, these nuclei are the ^{29}Si nucleus for $R \to 0$ and the ^{13}C and ^{16}O nuclei for $R \to \infty$. First, we consider the ^{16}O and ^{29}Si nuclei, which are assumed to have spherical shapes. The single-particle states of these nuclei are described by a spherical potential and a spin-orbit term:

$$V = -V_0(1+ar^2)\exp(-r^2/\lambda^2) + \frac{4V_0\kappa}{M\hbar\omega_0}\frac{d}{dr^2}[(1+ar^2)\exp(-r^2/\lambda^2)]\mathbf{l}\cdot\mathbf{s} \,. \quad (22)$$

The energy $\hbar\omega_0$ appearing in the spin-orbit term is set as $\hbar\omega_0 = 41A^{-1/3}$ MeV. In order to solve the eigenvalue problem, we have chosen the oscillator states (11) as basis set up to the fourth or fifth shell ($N = n_1 + n_2 + n_3 = 3$ or 4) and varied the oscillator length $\Lambda(\Lambda_1 = \Lambda_2 = \Lambda_3)$. Figure 2 shows the lowest single-particle energies of ^{16}O as a function of $\hbar\omega = \hbar^2/(M\Lambda^2)$ for $N = 3$. We note that the best value for $\hbar\omega$ is obtained as $\hbar\omega = 12$ MeV in this case. The same variational procedure is carried out in all calculations presented here.

Figure 3 shows the potentials and the experimental and calculated neutron single-particle energies of ^{16}O and ^{29}Si. The experimental single-particle energies are taken from Refs. 29 and 30. The potential parameters V_0, a, λ, and κ are determined by fitting the experimental single-particle energies around the Fermi level. The calculated energies of the deepest bound states lie as usually too high and give too small binding energies. The values of the parameters of the potentials and the energy quantum $\hbar\omega$ used for the basis oscillators are listed in Table I. Calculations with different basis sets up to the fourth and fifth shells ($N = 3$ and 4) have shown that the basis set including all states up to the fourth shell is already sufficiently large enough to represent the lowest eigenenergies correctly.

The ^{13}C nucleus can be considered to consist of a ^{12}C

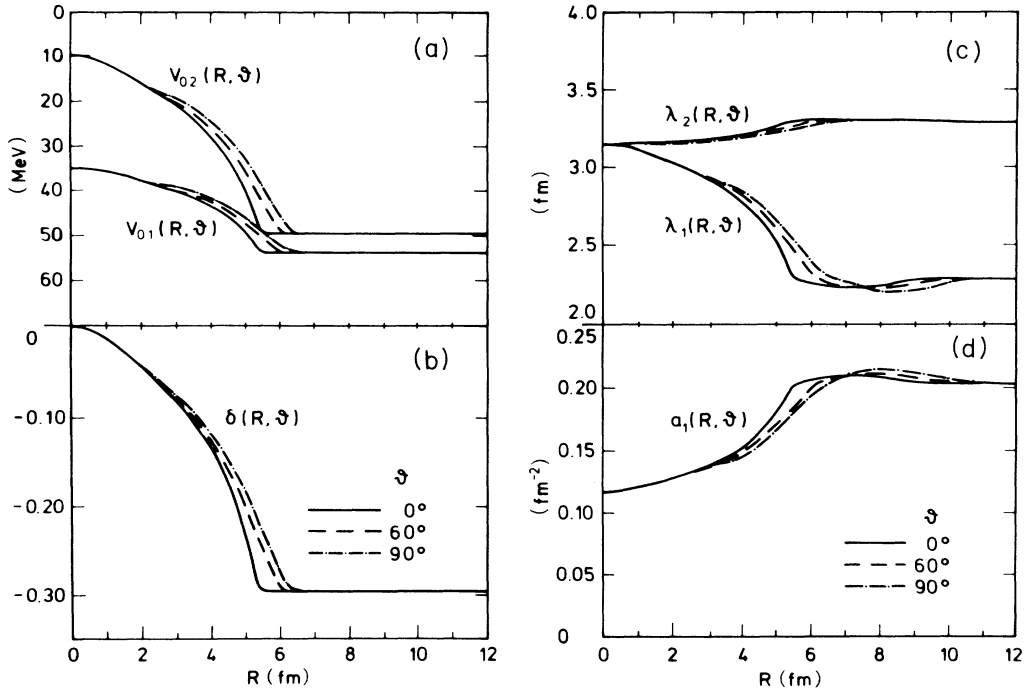

FIG. 7. The parameters (a) V_{0i}, (b) δ, (c) λ_i, and (d) a_1 of the TCSM potential for $^{16}O + {}^{13}C$ as a function of R for the orientation angles $\theta = 0°$ (solid curves), 60° (dashed curves), and 90° (dotted-dashed curves) of the symmetry axis of ^{13}C.

core and a weakly bound valence neutron. Whereas the ^{12}C nucleus is strongly deformed with an oblate shape, this deformation is reduced for ^{13}C by the extra particle. Therefore, the spectrum of ^{13}C can be described either by weak-coupling models with spherical single-particle states or by strong-coupling models where the ^{12}C core provides a deformed mean potential for the valence neutron (for literature, see Refs. 31–33). We have used the latter procedure in the present work.

Table II gives the energies and spins of the three lowest ^{13}C states which are assumed to be the heads of the lowest rotational bands. The energies of the rotational states can be calculated by the formula given by Eisenberg and Greiner:[26]

$$E_{IK}=\epsilon_{\Omega=K}+(\hbar^2/2J)[\,I(I+1)-2K^2 +\delta_{K,1/2}d(-1)^{I+1/2}(I+\tfrac{1}{2})]\ . \quad (23)$$

Here, ϵ_Ω is the single-particle energy, d the decoupling parameter, and K and Ω the quantum numbers of the components of the total and single-particle angular momenta along the body-fixed axis, respectively. In order to obtain the values of the neutron single-particle energies $\epsilon_{\Omega=K}$, we have set the energy of the ground state of ^{13}C to be equal to the negative value of the neutron separation energy, i.e., $E_{I=1/2\,K=1/2}=-4.95$ MeV. The single-particle energies are obtained according to Eq. (23) by using the experimental energies of the ^{13}C states.[29] The resulting "experimental" single-particle energies, as listed in Table II, are used to fit the shell model potential. We assumed the following shape of the deformed potential:

$$V=-V_0\exp[-(\delta_x^2x^2+\delta_y^2y^2+\delta_z^2z^2)/\lambda^2] +\frac{2V_0\kappa}{M\hbar\omega_0}\{\nabla\exp[-(\delta_x^2x^2+\delta_y^2y^2+\delta_z^2z^2)/\lambda^2]\times\mathbf{p}\}\cdot\mathbf{s}\ , \quad (24)$$

where $\delta_x=\delta_y$ and δ_z depend on the deformation parameter δ according to Eqs. (6) and (7). The parameters $V_0,\lambda,\delta,\kappa$ fitting the "experimental" single particle energies and $\hbar\omega$ of the basis set ($\hbar\omega_x=\hbar\omega_y=\hbar\omega\delta_x$, $\hbar\omega_z=\hbar\omega\delta_z$) are given in Table I. Figure 4 shows the potential of ^{13}C along the x and z axes, and Fig. 5 the dependence of the eigenvalues on the deformation parameter δ and a comparison with the "experimental" single-particle energies. The obtained oblate deformation parameter of $\delta=-0.3$ for ^{13}C is smaller than the one known for ^{12}C, indicating that the weak-coupling models can also explain the experimental spectrum of ^{13}C.

B. The TCSM potential for ^{13}C + ^{16}O → ^{29}Si

The parameters of the potential, found for $R\to0$ and $R\to\infty$ as tabulated in Table I, have to be interpolated for finite values of R. This interpolation cannot uniquely be carried out. For simplicity, we have assumed the potential to be in the form of Eq. (2) with

$$V_1=-V_{01}(1+a_1r^2)\exp(-r^2/\lambda_1^2)\ , \quad (25)$$

$$V_2=-V_{02}\exp[-(\delta_{x'}^2x'^2+\delta_{y'}^2y'^2+\delta_{z'}^2z'^2)/\lambda_2^2]\ , \quad (26)$$

where

$$x'=-(z-R)\sin\theta+x\cos\theta\ ,$$
$$y'=y\ , \quad (27)$$
$$z'=(z-R)\cos\theta+x\sin\theta\ .$$

As shown in Fig. 6, the centers of the ^{16}O and ^{13}C nuclei are fixed at the coordinate origin and at $z=R$, respectively. The intrinsic z' axis of the ^{13}C nucleus is rotated by the angle θ around the y axis with respect to the z axis.

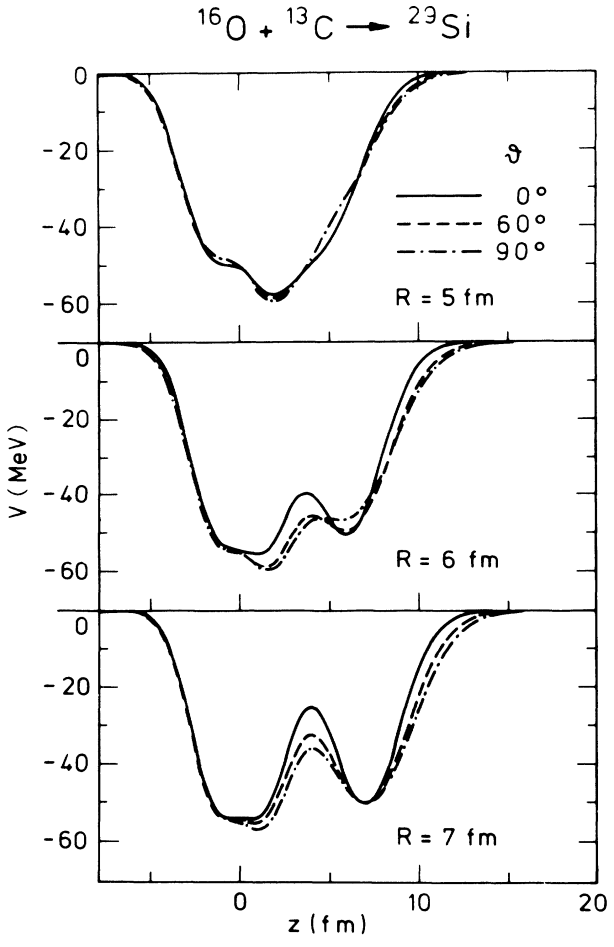

FIG. 8. Cut of the TCSM potential of ^{16}O + ^{13}C along the internuclear axis (z axis) for the relative distances $R=5$, 6, and 7 fm and the orientation angles $\theta=0°$ (solid curves), 60° (dashed curves), and 90° (dotted-dashed curves) of the symmetry axis of ^{13}C. The ^{16}O nucleus is centered at $z=0$, the ^{13}C nucleus at $z=R$.

The transformation between the coordinates x,y,z and x',y',z' is given by Eq. (27).

The potential parameters $V_{0i},\lambda_i,a_1,\delta_{x'},\delta_{y'},\delta_{z'}$ and spin-orbit parameters C_i are functions of R and θ. The deformation parameters are expressed in terms of $\delta(R,\theta)$ according to Eqs. (6) and (7). First, we tried to reduce the interpolation by introducing a single unknown function $f(R,\theta)$ as follows ($i=1,2$):

$$A(R,\theta)=A(R=0)[1-f(R,\theta)]+A(R\rightarrow\infty)f(R,\theta)\ , \tag{28}$$

where A stands for the parameters V_{0i}, λ_i, a_1, δ, and C_i, respectively, and the function $f(R,\theta)$ depends on R and θ and satisfies the boundary conditions

$$f(R=0,\theta)=0,\quad f(R\rightarrow\infty,\theta)=1\ . \tag{29}$$

The values of the parameters are not uniquely determined at $R=0$ by the parameters of the ^{29}Si potential. We choose the following partition of the parameters between the two potentials V_1 and V_2:

$$\begin{aligned} &V_{01}(R=0)=35\ \text{MeV},\quad V_{02}(R=0)=10\ \text{MeV}\ ,\\ &\lambda_1(R=0)=\lambda_2(R=0)=3.15\ \text{fm}\ ,\\ &\delta(R=0)=0\ ,\\ &C_1(R=0)=C_2(R=0)=C(^{29}\text{Si})\ . \end{aligned} \tag{30}$$

The parameter $a_1(R=0)$ is then fixed by $V_{01}(R=0)$ and the form of the ^{29}Si potential. The chosen ratio between $V_{01}(R=0)$ and $V_{02}(R=0)$ leads to single-particle energies for small values of R as they are found for small quadrupole deformations in the Nilsson model (see Sec. IV C).

The function $f(R,\theta)$ is determined by the volume conservation condition (9) with $V_0=-10$ MeV. This is possible up to a critical value $R_c(\theta)$ with $R_c(\theta=0°)=5.75$ fm and $R_c(\theta=90°)=6.50$ fm. For $R\geqq R_c(\theta)$ we have set the parameters V_{0i} and δ equal to their asymptotic values and the parameters λ_i, a_1, and C_i varied according to Eq. (28) by using again the volume conservation condition (9) with $V_0=-10$ MeV. The resulting parameters of the two-center potential are shown in Fig. 7 as a function of R for different angles θ.

Figure 8 shows the two-center potential along the z axis for the relative distances $R=5$, 6, and 7 fm and the orientation angles $\theta=0°$, 60°, and 90° of the symmetry axis of ^{13}C. Figure 9 presents the equipotential surfaces for $R=4$, 6, 8, and 10 fm and a fixed orientation angle of $\theta=60°$. It is seen that the potential is nearly independent of the ^{13}C orientation for relative distances $R\leqq 5$ fm. For larger relative distances, $R>5$ fm, the barrier between the potentials of ^{13}C and ^{16}O is smallest for $\theta=90°$ as expected. Only in the case of $\theta=0°$ the potential is rotationally symmetric about the internuclear axis (z axis).

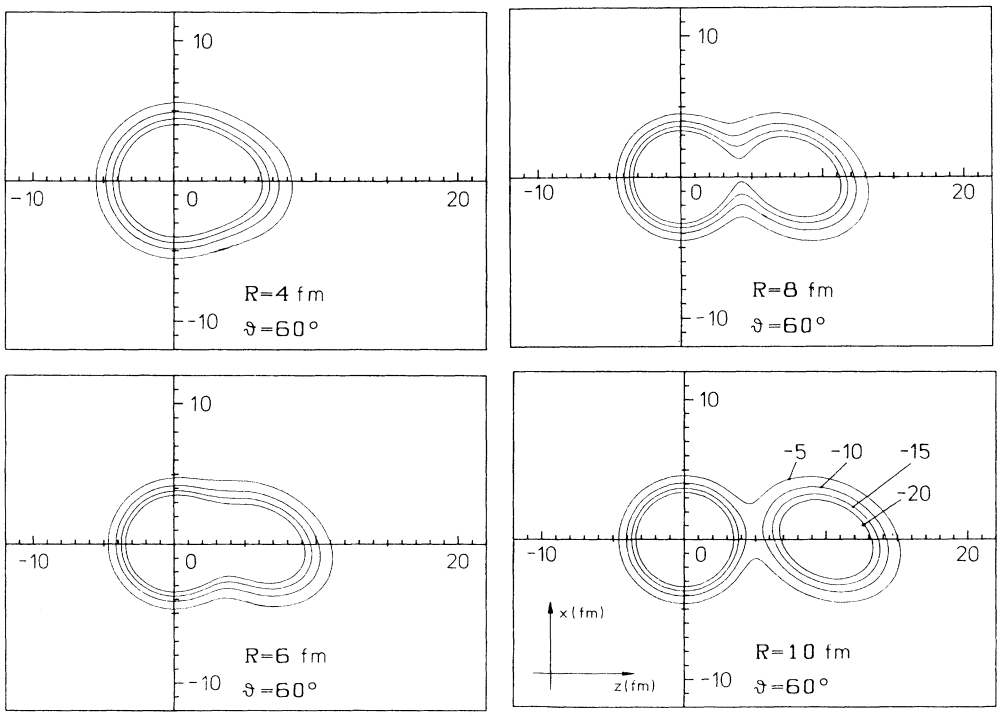

FIG. 9. Equipotential surfaces of the TCSM potential of ^{16}O + ^{13}C with $V=-5$, -10, -15, and -20 MeV in the x-z plane for relative distances $R=4$, 6, 8, and 10 fm and an orientation angle $\theta=60°$.

C. Level diagram for $^{13}C + {}^{16}O \rightarrow {}^{29}Si$

The diagonalization of the TCSM Hamiltonian has been done with oscillator basis functions centered at the centers of ^{16}O and ^{13}C. The oscillator functions centered at $z=0$ are isotropic with $\hbar\omega_x=\hbar\omega_y=\hbar\omega_z=\hbar\omega_1(R)$ and the ones centered at $z=R$ have $\hbar\omega_{x'}=\hbar\omega_{y'}=\hbar\omega_2(R)\delta_{x'}$ and $\hbar\omega_{z'}=\hbar\omega_2(R)\delta_{z'}$. The values of $\hbar\omega_i(R)$ are obtained by a variational calculation with a rotationally symmetric TCSM potential for spherical nuclei. For each center all 20 oscillator functions with $N\leqq 3$ have been taken into account.

Figure 10 shows the TCSM level diagram as a function of R for $\theta=0°$. Due to the rotational symmetry of the potential about the internuclear axis, only in this special case can the levels be classified with the quantum number Ω of the projection of the angular momentum on the internuclear axis. For $R\rightarrow\infty$, the ^{13}C levels show the Nilsson spectrum of an oblately deformed potential. For $R\rightarrow 0$ the TCSM levels approach the spectrum of ^{29}Si. A similar level diagram for the same system, but with spherical shapes of the nuclei for $R\rightarrow\infty$, was calculated by Park *et al.*[20]

Level diagrams as a function of θ are shown for fixed two-center distances $R=6$ and 7 fm in Fig. 11. The lev-

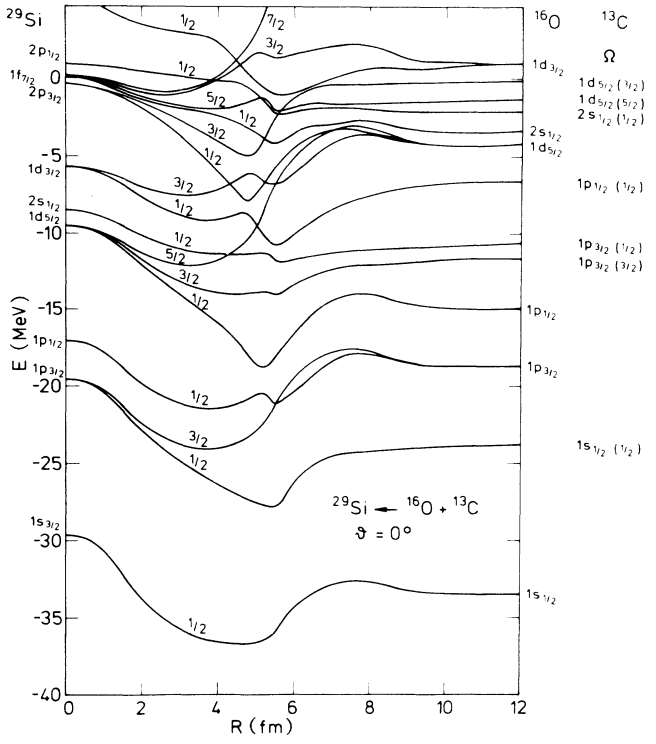

FIG. 10. The single-particle level diagram of the TCSM for $^{16}O + {}^{13}C \rightarrow {}^{29}Si$ as a function of R for $\theta=0°$. In this case the potential is rotationally symmetric about the internuclear axis. For each level the quantum number Ω of the projection of angular momentum on the internuclear axis is indicated. Also, the spectroscopic notations of the ^{29}Si, ^{16}O, and ^{13}C levels are given for $R=0$ and $R\rightarrow\infty$.

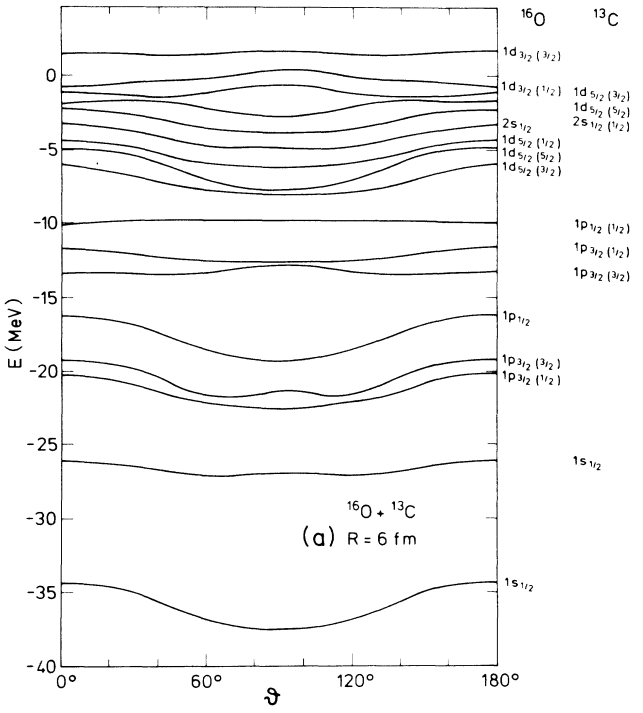

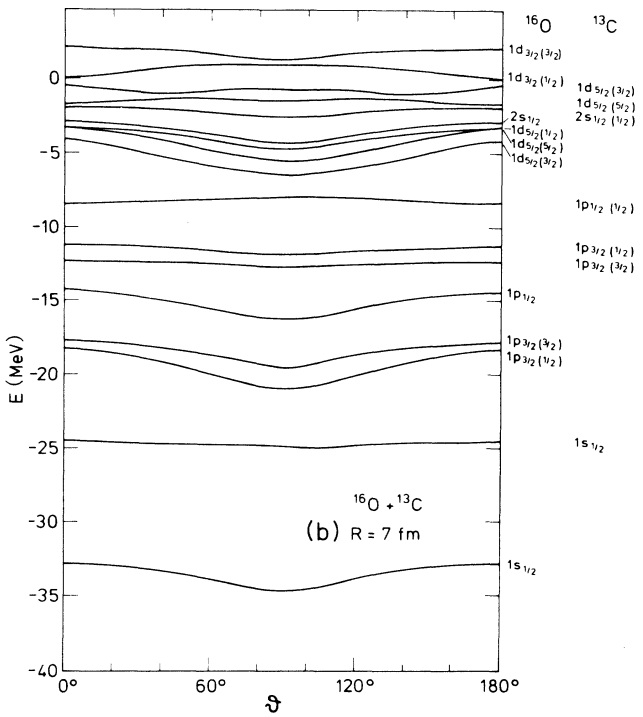

FIG. 11. The single-particle level diagram of the TCSM for $^{16}O + {}^{13}C \rightarrow {}^{29}Si$ as a function of the orientation angle θ of the symmetry axis of ^{13}C for (a) $R=6$ fm and (b) $R=7$ fm. The levels are denoted by their asymptotic ($R\rightarrow\infty$) quantum numbers for $\theta=0°$.

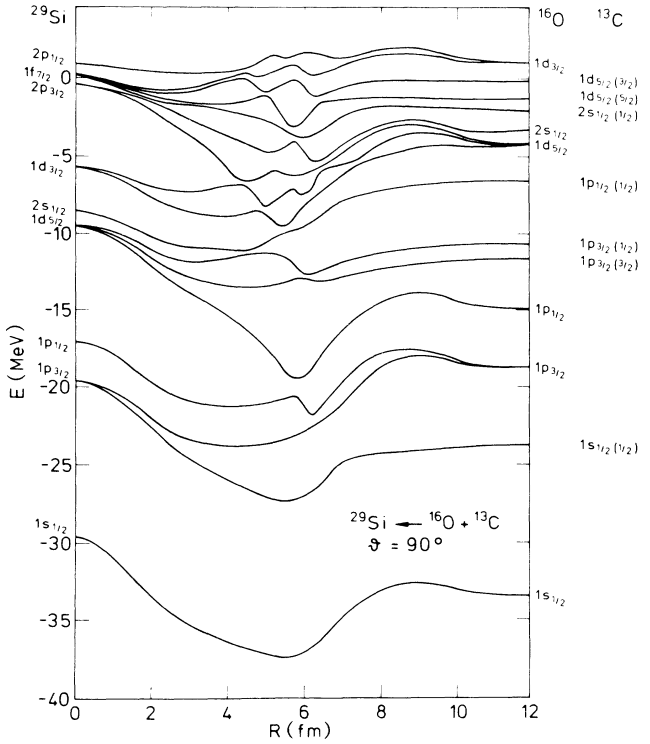

FIG. 12. The single-particle level diagram of the TCSM for $^{16}O + {}^{13}C \rightarrow {}^{29}Si$ as a function of R for $\theta = 90°$.

els are twofold degenerate because of the invariance of the Hamiltonian with respect to a reflection on the plane spanned by the nuclear symmetry axis of ^{13}C and the internuclear axis. The levels are denoted by their asymptotic ($R \rightarrow \infty$) quantum numbers for $\theta = 0°$.

It is quite interesting to note that the $1d_{5/2}$ levels of ^{16}O are lowered for $\theta = 90°$, whereas the $1p_{1/2}$ level of ^{13}C is nearly unaffected by the orientation angle. Orientations with extreme values of the energy difference between two levels are preferentially found at the angles $\theta = 0°$ and 90°. For example, it is seen in Fig. 11(b) that the energy difference between the $1d_{5/2}$ ($\Omega = \frac{3}{2}$) level of ^{16}O and the $1p_{1/2}$ level of ^{13}C drops from 4.3 MeV at $\theta = 0°$ to 1.6 MeV at $\theta = 90°$.

For $\theta = 0°$ the potential is rotationally symmetric and, therefore, the levels with different values of the magnetic quantum number Ω can cross each other. This is different for $\theta \neq 0$ as shown in Fig. 12 for $\theta = 90°$, where no level crossings occur for $0 < R < \infty$. The reminder of the crossings of levels with different values of Ω for $\theta = 0$ are the additional avoided crossings. For example, the lowest $1d_{5/2}$ ($\Omega = \frac{5}{2}$) level has no crossing for $\theta \neq 0$, but several avoided crossings. At the points of avoided crossings, transitions between the corresponding levels can preferentially take place with large transition strengths. They can be considered as Landau-Zener–type promotion processes for loosely bound neutrons.

V. CONCLUSIONS

The new TCSM we have developed in this paper can be used to predict and interpret reactions between deformed nuclei. The dependence of TCSM levels on the orientation of the deformed nuclei leads to enhancements of selected single-particle reactions for certain relative orientations of the intrinsic axes.

In a microscopic molecular reaction theory based on the states (10) of the new TCSM, three types of transition matrix elements between the molecular single-particle states are essential for the reactions: the radial matrix elements ($\sim \partial/\partial R$), the rotational matrix elements dependent on the total angular momentum operator, and the matrix elements measuring the orientation of the intrinsic nuclear axes and which are dependent on the angular momenta of the nuclei (fragments) ($\sim \mathbf{I}_1, \mathbf{I}_2$). In the case of the $^{13}C + {}^{16}O$ reaction, the last matrix elements have to be calculated as $\langle \psi_i \mid \partial/\partial\theta \mid \psi_j \rangle$ and measure the change of the molecular states with the orientation of the symmetry axis of ^{13}C. Similar arguments as used for the enhancement of transitions due to the radial coupling at avoided level crossings (Landau-Zener effect) can be applied for the avoided level crossings as a function of the orientation angles of the nuclei. Therefore, we expect enhanced transitions at these avoided crossings as a new effect.

In order to study the consequences of the new TCSM for reactions between deformed nuclei in more detail, a microscopic molecular reaction theory has first to be developed which uses molecular single-particle states between deformed nuclei. Such a theory has not yet been formulated in nuclear physics to our knowledge, but is needed for the interpretation of reactions between light deformed and polarized nuclei (see, for example, Ref. 34).

This work was supported by the Bundesministerium für Forschung und Technologie and the Gesellschaft für Schwerionenforschung (Darmstadt).

[1]P. Holzer, U. Mosel, and W. Greiner, Nucl. Phys. **A138**, 241 (1969).
[2]D. Scharnweber, W. Greiner, and U. Mosel, Nucl. Phys. **A164**, 257 (1971).
[3]J. A. Maruhn and W. Greiner, Z. Phys. **251**, 431 (1972).
[4]J. A. Maruhn, W. Greiner, and W. Scheid, in *Heavy Ion Collisions*, edited by R. Bock (North-Holland, Amsterdam, 1980), Vol. 2, Chap. 6, p. 397.
[5]K. Pruess and W. Greiner, Phys. Lett. **33B**, 197 (1970).
[6]U. Mosel, T. D. Thomas, and P. Riesenfeldt, Phys. Lett. **33B**, 565 (1970).
[7]J. Y. Park, W. Scheid, and W. Greiner, Phys. Rev. C **6**, 1565 (1972).
[8]W. von Oertzen and W. Nörenberg, Nucl. Phys. **A207**, 113

(1973).
[9]F. Becker, S. Joffily, C. Beccaria, and G. Baron, Nucl. Phys. **A221**, 475 (1974).
[10]Review and further references: R. J. Ascuitto and E. A. Seglie, in *Treatise on Heavy-Ion Science,* edited by D. A. Bromley (Plenum, New York, 1984), Vol. 1.
[11]Review and further references: B. Imanishi and W. von Oertzen, INS Report 586, Institute for Nuclear Study, University of Tokyo, Tanashi, Tokyo, 1986.
[12]R. W. Hasse, Ann. Phys. (N.Y.) **80**, 118 (1971).
[13]S. K. Korotky, K. A. Erb, R. L. Phillips, S. J. Willett, and D. A. Bromley, Phys. Rev. C **28**, 168 (1983).
[14]R. M. Freeman, C. Beck, F. Haas, B. Heusch, and J. J. Kolata, Phys. Rev. C **28**, 437 (1983).
[15]C. Beck, R. M. Freeman, F. Haas, B. Heusch, and J. J. Kolata, Nucl. Phys. **A443**, 157 (1985).
[16]R. M. Freeman, C. Beck, F. Haas, A. Morsad, and N. Cindro, Phys. Rev. C **33**, 1275 (1986).
[17]G. Terlecki, W. Scheid, H. J. Fink, and W. Greiner, Phys. Rev. C **18**, 265 (1978).
[18]R. Könnecke, W. Greiner, and W. Scheid, Phys. Rev. Lett. **51**, 366 (1983).
[19]B. Imanishi, W. von Oertzen, and H. Voit, INS Report 585, Institute for Nuclear Study, University of Tokyo, Tanashi, Tokyo, 1986.
[20]J. Y. Park, W. Greiner, and W. Scheid, Phys. Rev. C **21**, 958 (1980).
[21]Y. Abe and J. Y. Park, Phys. Rev. C **28**, 2316 (1983).
[22]B. Milek and R. Reif, Phys. Lett. **157B**, 134 (1985).
[23]N. Cindro, R. M. Freeman, and F. Haas, Phys. Rev. C **33**, 1280 (1986).
[24]J. Y. Park, K. Gramlich, W. Scheid, and W. Greiner, Phys. Rev. C **33**, 1674 (1986).
[25]S. G. Nilsson, K. Dansk. Vidensk. Selsk. Mat.-Fys. Medd. **29**, No. 16 (1955).
[26]J. M. Eisenberg and W. Greiner, *Nuclear Theory* (North-Holland, Amsterdam, 1970), Vol. 1.
[27]G. Nuhn, diploma thesis, University of Giessen, 1986 (unpublished).
[28]J. Y. Park, W. Scheid, and W. Greiner, Phys. Rev. C **25**, 1902 (1982).
[29]F. Ajzenberg-Selove, Nucl. Phys. **A268**, 1 (1976); **A281**, 1 (1977).
[30]P. M. Endt and C. van der Leun, Nucl. Phys. **A310**, 1 (1978).
[31]D. Kurath and R. D. Lawson, Nucl. Phys. **23**, 5 (1961).
[32]S. Cohen and D. Kurath, Nucl. Phys. **73**, 1 (1965); **A101**, 1 (1967).
[33]J. T. Reynolds, C. J. Slavik, C. R. Lubitz, and N. C. Francis, Phys. Rev. **176**, 1213 (1968).
[34]Heidelberg-Marbug-Warsaw Cooperation on Polarized Heavy Ions, Contributions to the 6th International Symposium on Polarization Phenomena in Nuclear Physics, Osaka, Japan, 1985, available as Max-Planck-Institut für Kernphysik, Heidelberg, Report MPI-H-1985-v16, 1985.